

# Comparative Study About Preparation of Poly(lactide)/Organophilic Montmorillonites Nanocomposites Through Melt Blending or Ring Opening Polymerization Methods

Stefania Castiello,<sup>1</sup> Maria-Beatrice Coltelli,<sup>1,2</sup> Lucia Conzatti,<sup>3</sup> Simona Bronco<sup>4</sup>

<sup>1</sup>Dipartimento di Chimica e Chimica Industriale (DCCI), Via Risorgimento 35, 56126 Pisa, Italy

<sup>2</sup>SPIN-PET s.r.l., Via Rinaldo Piaggio 32, 56025, Pontedera (Pisa), Italy

<sup>3</sup>CNR-ISMAR UOS Genova, Via de Marini 6, 16149 Genova, Italy

<sup>4</sup>IPCF-CNR, via G. Moruzzi 1, I-56124 Pisa, Italy

Received 6 April 2011; accepted 8 October 2011

DOI 10.1002/app.36313

Published online 20 January 2012 in Wiley Online Library (wileyonlinelibrary.com).

**ABSTRACT:** The present article is focused onto the study of nanostructure, thermal and mechanical properties of nanocomposites composed of poly(lactide) (PLA), and a constant amount of montmorillonite (MMT) clays (3 wt %). Properly modified organoclays with easily available commercial compounds were prepared in order to allow the homogeneous dispersion of the hydrophilic clays in the polar polymer matrix; in particular, 2-hydroxyethyl-trimethylammonium (choline), polyethyleneoxide(15)-(hydrogenated tallow)-ammonium, and oligochitosan salts were used as surfactants as their structure can match the requirements of a biocompatible material. These organi-

cally modified MMTs (OMMTs) were used for preparing composites by melt blending or by *in situ* ring opening polymerization (using the clay surfactant as polymerization initiator) followed by melt dispersion into a PLA matrix. Structural, morphological, and thermo-mechanical properties of the products are compared in order to assess advantages and disadvantages of the two different preparation routes. © 2012 Wiley Periodicals, Inc. *J Appl Polym Sci* 125: E413–E428, 2012

**Key words:** nanocomposites; PLA; montmorillonite

## INTRODUCTION

Poly(lactic acid) or poly(lactide) (PLA) is gaining much attention on behalf of both academy and industry<sup>1</sup> as it can provide biodegradable materials<sup>2</sup> with a good balance of physicochemical properties starting from renewable resources.<sup>3,4</sup> Hence, in attempt to finely modulate its mechanical, thermal, and gas barrier properties, its blends<sup>5</sup> and composites<sup>6,7</sup> are also the object of many investigations.

Among the inorganic additives, layered silicates such as montmorillonite (MMT) appear to be effective fillers to improve the overall performances of PLA system even at low concentration (1–5 wt %).<sup>8</sup> However, to reach this improvement, a high degree of clay dispersion that highly depends on the adopted preparation method and on the compatibility between the polymer matrix and the clay is needed.

In the case of polyesters-based nanocomposites different preparative methods can be adopted. One of the more interesting exploits the possibility to synthesize biodegradable polyesters, such as PLA and poly( $\epsilon$ -caprolactone) (PCL), via ring opening polymerization (ROP) reaction of the corresponding lactones.<sup>9,10</sup>

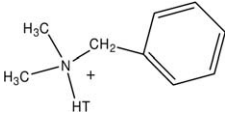
In particular, PLA can be synthesized either by ROP starting from the cyclic dimer, the lactide (3,6-dimethyl-1,4-dioxane-2,5-dione), or by condensation polymerization of lactic acid or its derivatives. In terms of molecular weight control, the living ROP of lactide yields a linear relationship between monomer conversion and molecular weight of PLA with low polydispersity index ( $\overline{M}_w/\overline{M}_n$ ). Moreover, ROP in conjunction with a “living” method have enabled the controlled synthesis of block, graft, and star polymers,<sup>11</sup> representing a powerful and versatile method of addition-polymerization. The most widely used initiators include alcohols and various aluminum and tin alkoxides and carboxylates. A catalyst is also added to favor the nucleophilic attack of initiator and hydroxyl terminated growing chain onto the cyclic monomer. Many attempts are reported in the synthesis of specific catalysts able to give a better control of structure<sup>12</sup> and stereoregularity properties.<sup>13,14</sup> Sn(2-ethylhexanoate)<sub>2</sub> was the largely adopted because it is commercially available,

Correspondence to: M.-B. Coltelli (beacolts@ns.dcci.unipi.it).

Contract grant sponsor: MIUR; contract grant number: PRIN 2008 Prot. 200898KCKY.

Contract grant sponsor: RiGePlast; contract grant number: Tuscany Region – POR CREO FESR 2007–2013.

**TABLE I**  
**Structure of Commercial Montmorillonites Employed for the Preparation of Biodegradable Polyesters Based Nanocomposites**

	Formula of the cation	Commercial name
Sodium montmorillonite	$\text{Na}^+$	Cloisite Na+ Dellite HPS
Methyl, tallow, bis-2-hydroxyethyl, quaternary ammonium montmorillonite	$\begin{array}{c} \text{CH}_2\text{CH}_2\text{OH} \\   \\ \text{CH}_3 - \text{N}^+ - \text{T} \\   \\ \text{CH}_2\text{CH}_2\text{OH} \end{array}$ <p>T is Tallow (~65% C18; ~30% C16; ~5% C14)</p>	Cloisite 30 B
Dimethyl, benzyl, hydrogenated tallow, quaternary ammonium montmorillonite	 <p>HT is Hydrogenated Tallow</p>	Cloisite 10A Dellite 43B
Dimethyl, dehydrogenated tallow, 2-ethylhexyl quaternary ammonium montmorillonite	$\begin{array}{c} \text{CH}_3 \\   \\ \text{CH}_3 - \text{N}^+ - \text{CH}_2\text{CHCH}_2\text{CH}_2\text{CH}_2\text{CH}_3 \\   \quad   \\ \text{HT} \quad \text{CH}_3 \end{array}$	Cloisite 25A
Methyl, dehydrogenated tallow, quaternary ammonium montmorillonite	$\begin{array}{c} \text{H} \\   \\ \text{CH}_3 - \text{N}^+ - \text{HT} \\   \\ \text{HT} \end{array}$	Cloisite 93A
Dimethyl, dehydrogenated tallow, quaternary ammonium montmorillonite	$\begin{array}{c} \text{CH}_3 \\   \\ \text{CH}_3 - \text{N}^+ - \text{HT} \\   \\ \text{HT} \end{array}$	Cloisite 20A (0.95 mg/g clay) Cloisite 15A (1.25 mg/g clay) Cloisite 6A (1.4 mg/g clay) Dellite 72T

easy to be handled, and soluble in common organic solvents and in melt monomers.<sup>15</sup> It is highly active (typical reaction times in bulk at 140–180°C range from minutes to a few hours) and allows the preparation of high-molecular-weight polymers (up to 10<sup>5</sup> or even 10<sup>6</sup> Da in the presence of an alcohol).<sup>11</sup>

Only in few articles, the ROP of biodegradable polyesters was also performed in the presence of montmorillonites (MMTs). Both, Kubies et al.<sup>16</sup> and Lepoittevin et al.<sup>17,18</sup> studied the ROP of  $\epsilon$ -caprolactone ( $\epsilon$ -CL) in the presence of modified MMTs. PCL-grafted layered silicate nanohybrids were thus prepared according to a controlled coordination–insertion mechanism by using aluminum- or tin-based catalysts. More recently, Chrissafis et al.<sup>19</sup> prepared PCL nanocomposites by following a similar approach, but using Ti(OBu)<sub>4</sub> as coordination–insertion catalyst. However, only two papers reported on the preparation of PLA-based nanocomposites by using this method. For example, Paul et al.<sup>20</sup> synthesized PLA/layered aluminosilicate nanocomposites by ROP, using two different types of organo-montmor-

illonites (OMMTs) (Cloisite 30B and Cloisite 25A, see Table I). When Cloisite 30B was used, the polymerization was co-initiated by AlEt<sub>3</sub> and the growing polymer chains were directly “grafted” onto the clay surface through the hydroxyl-functionalized ammonium cations, yielding exfoliated nanocomposites with enhanced thermal stability.

A similar result was obtained more recently by Lee,<sup>21</sup> who modified the surface of Cloisite 30B by grafting low-molecular-weight PLA chains ( $M_n$  9,400–21,600) through the *in situ* polymerization approach involving the preliminary activation of hydroxyl sites with Sn(2-ethylhexanoate)<sub>2</sub>. The composite obtained was then melt-blended with a high-molecular-weight PLA matrix. This novel clay/PLA nanocomposite showed a high shear-thinning behavior when the molecular weight of the grafted PLA was higher than the critical molecular weight of chain entanglement.

However, melt intercalation has attracted, until now, more attention than other processes because of its economic and practical advantages. In the last

decade, the influence of different parameters on clay dispersion was analyzed. Di et al.<sup>22</sup> mixed two different OMMTs (Cloisite 30B and Cloisite 93A, see Table I) in PLA matrix by using an internal mixer. It was observed that only the Cloisite 30B gave exfoliated nanocomposites. The results obtained by Feijo et al.,<sup>23</sup> that compared composites containing two commercial OMMTs, namely Dellite 43B and Dellite 72T (see Table I), showed that the former interacted more strongly with PLA. A better dispersion of the organoclay in the PLA matrix and a slightly higher thermal stability was observed. PLA/Dellite 72T composites showed only aggregates of micrometric dimensions. Hence, replacement in the modifier chemical structure of a long alkyl chain (hydrogenated tallow) with an aromatic ring improves the affinity of the MMT with the PLA matrix. This result could, however, be ascribed to the higher polarity of the Dellite 43B ammonium salt. Pluta et al.<sup>24–26</sup> investigated the effect of the processing conditions by preparing PLA/phyllsilicates composites containing 3 wt % of Cloisite 30B in a discontinuous laboratory mixer. In particular, the influence of blending time (6.5, 10, 20, and 30 min) and rotor speed (50 and 100 rpm) on the morphology and properties of the nanocomposites was investigated. Whilst the molecular weight was marginally reduced by increasing the blending time, the level of dispersion of the filler into the matrix was improved and, despite of the relatively low content of clay, final properties were remarkably affected by the presence of OMMT.

It is known that many factors affect the chemical behavior of PLA during melt processing, including the grade of PLA used, the processing conditions applied (temperature, rotation speed, residence time, atmosphere, drying efficiency of the components), and the presence of additives and their chemical nature. Moreover, the rheological properties of the nanocomposites, as determined during a dynamic frequency sweep, appeared to be very sensitive to the nanostructure evolution.<sup>27,28</sup>

The present article deals with preparation and study of nanostructure, thermal and mechanical properties of nanocomposites based on PLA and a constant amount of organoclay (3 wt %).<sup>24–26</sup> OMMTs were prepared by ionic exchange by using proper commercial ammonium salts in order to allow the homogeneous dispersion of the hydrophilic clays in the polyester matrix; in particular, 2-hydroxyethyl-trimethylammonium (choline), polyethyleneoxide(15)-(hydrogenated tallow)-ammonium, and oligochitosan salts were selected as surfactants, because their structure can match the requirements of a biocompatible material. The OMMTs were used for preparing composites by two different methods, that is melt blending and *in situ* ROP (using the clay surfactant as initiator for the polymerization) fol-

lowed by melt dispersion into a PLA matrix. Structural, morphological, and thermo-mechanical properties of the products were compared in order to assess advantages and disadvantages of the use of different organically modified clays and of the two different preparation routes.

## EXPERIMENTAL

### Materials

PLA Polymer 2002D (density 1.24 g/cm<sup>3</sup>;  $\overline{M}_n = 120,000$ ;  $\overline{M}_w = 111,000$ ;  $T_g = 60.1^\circ\text{C}$ ) was a NatureWorks product (Natureworks BV, Naarden, Netherlands).

The organo-modified clays (OMMT) were prepared by cationic exchange of a natural MMT kindly supplied by Laviosa Chimica Mineraria (Livorno, Italy), having an average size of 8  $\mu\text{m}$  and interlayer distance, determined by X-ray diffraction, of 1.24 nm. Pyrophyllite was supplied by Maffei Natural Resources (Reggio Emilia, Italy). Four different types of alkylammonium salts were used to increase the surface hydrophobicity of pristine MMT: 2-hydroxyethyl-trimethylammonium chloride (choline chloride) (Sigma-Aldrich, Milano, Italy, assay > 97%), choline lactate (Sigma-Aldrich, assay > 95%), polyethyleneoxide(15)-(hydrogenated tallow)-ammonium chloride (Ethoquad) (Akzo Nobel), and oligo(chitosan lactate) (Sigma-Aldrich, Reggio Emilia, Italy). The chemical structure of the surfactants is shown in Figure 1.

Cationic exchange capacity (CEC) of pristine montmorillonite was determined through a cationic exchange reaction with Methylene Blue (MB) (Sigma-Aldrich) and *p*-( $\beta$ -naphthol-azo)benzene sulfonate (Sigma-Aldrich, assay > 85%) was used for the determination of the ion-exchange reactions yields.

1-butanol (Carlo Erba, assay 99.5%) was dried on K<sub>2</sub>CO<sub>3</sub> and distilled under nitrogen atmosphere.

*Rac*-3,6-dimethyl-1,4-dioxane-2,5-dione (lactide) and Tin(II) octanoate were Sigma-Aldrich products (assay > 96% and 98%, respectively).

Phosphate buffered tablets for the hydrolytic degradation tests were purchased from Sigma-Aldrich.

### Preparation of the OMMTs

In order to determine the CEC of MMT-Na<sup>+</sup>, 50 mL of an aqueous 0.99M solution of Methylene Blue (MB) were dropwise added under continuous stirring to 2.5 mL of a 4.5% w/w clay suspension in a 100 mL polyethylene bottle. The final volume was brought to 100 mL. The bottle was sealed, kept at (25  $\pm$  2) $^\circ\text{C}$  under stirring. After an incubation time of 24 h, an aliquot of the suspension was filtered and the concentration of the MB was determined by measuring the absorption at 662 nm.

For the remainder of this article, the identification names MMT-Na<sup>+</sup>, MMT-Ch, MMT-Et, MMT-CC,

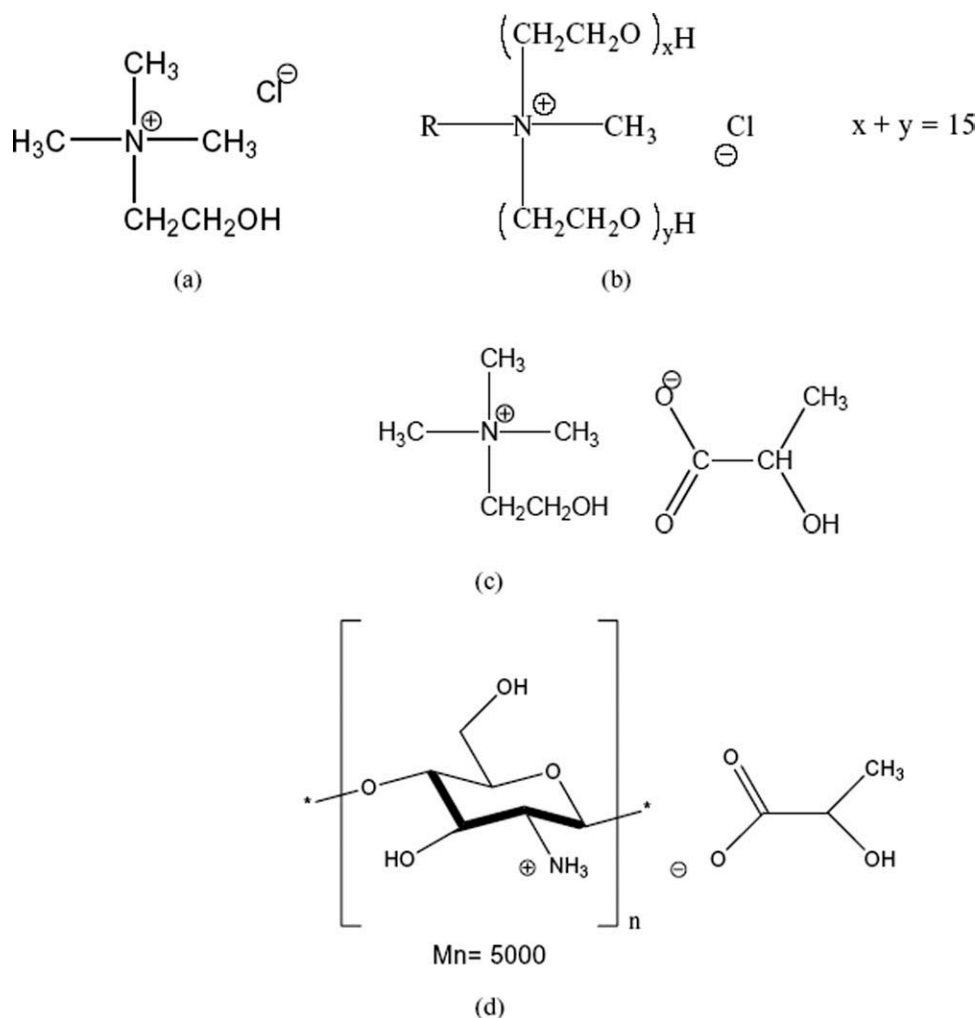


**Figure 1** Chemical structure of (a) 2-hydroxyethyl-trimethylammonium chloride (choline chloride), (b) polyethyleneoxide(15)-(hydrogenated tallow)-ammonium chloride (Ethoquad), (c) choline lactate, and (d) oligo(chitosan lactate).

MMT-CL will refer to the pristine montmorillonite and the modified montmorillonite with oligo(chitosan lactate), Ethoquad, choline chloride, and choline lactate, respectively. For the preparation of MMT-Ch, oligo(chitosan lactate) (6.6 mmol) was dispersed under stirring in a water suspension of MMT-Na<sup>+</sup> (140 mL, 4.5% w/w, CEC = 110 ± 5 meq/mol) at 60°C for 3 h. The resulting sludge was separated from the aqueous solution after centrifugation (5000 rpm, 10 min), washed with small amounts of water until the complete chloride removal and finally lyophilized. The same procedure was used for the preparation of MMT-Et and MMT-CC. To study the influence of the solvent polarity on the ion exchange reaction yield, the same procedure was repeated dispersing the alkylammonium salts in a water/propanol (50/50) suspension of MMT-Na<sup>+</sup>.

For the synthesis of MMT-CL, 6.6 g of MMT-Na<sup>+</sup> were directly suspended in 1.28 g of choline lactate. Four milliliter of the aqueous solution from the centrifugation, 1 mL of Orange II saturated solution,

and 5 mL of HPLC chloroform were added into glass test tubes, in order to determine the exchange degree. The tubes were shaken 100 times, centrifuged (4000 rpm, 5 min) and about 4 mL of the organic phase transferred to the spectrophotometer cells.

#### Preparation of composites by melt intercalation

After drying at 60°C for 3 h under reduced pressure, PLA pellets were melt-blended with the OMMTs (3% w/w of an inorganic fraction) in a counter-rotating internal mixer (Brabender type) at the constant rotation speed of 100 rpm for 20 min. Melt processing was carried out in a dry nitrogen atmosphere to prevent thermo-oxidative degradation of PLA. The temperature was set at 180°C. For the remainder of this article, the identification name PLA, NanoCL, nanoEt, nanoCC, and nanoCh will refer to the pure PLA and the composites obtained by melt blending

of MMT-CL, MMT-Et, MMT-CC, and MMT-Ch, respectively.

Composites containing 3 wt% of OMMTs, previously milled using a ball mill and sieved to obtain particles with an average size comparable to commercial clays, were prepared with a similar procedure. Neat PLA was also melt processed to prepare a reference material.

#### Preparation of nanohybrids by *in situ* intercalative polymerization

For the synthesis of PLA in the presence of OMMT, keeping into account the values of yield obtained for the ROP polymerization of lactide, 5.07 g of *rac*-lactide, 1.42 g of MMT-CC, previously dried under reduced pressure (100°C, 0.01 bar) for 12 h, and 10 mL of toluene were charged into a 50 mL, three-necked, round-bottom flask connected to a dry N<sub>2</sub> purge. An oil bath, thermostated to 95°C, was raised to entirely submerge the flask and the mixture was magnetically stirred. After the dissolution of lactide in toluene solvent and MMT-CC, 0.1 wt % of the Sn(Oct)<sub>2</sub> catalyst was transferred to the reaction kettle. The percent conversion of the reaction was monitored after 24 h by <sup>1</sup>H-NMR and FTIR on an aliquot of the mixture. The polymer was then precipitated from cold MeOH and the solid was isolated and dried *in vacuo* until constant weight.

The methanol-soluble polymer fraction was recovered by solvent removal.

The same procedure was adopted for the PLA synthesis in the presence of MMT-Et. The products were named MasterC and MasterE, respectively.

In order to assess the effect of phyllosilicates onto the product structure, pure PLA and PLA in the presence of MMT-Na<sup>+</sup> were synthesized. Pure PLA (sample PLA-Bu) was synthesized by the following procedure: 5.4 g of *rac*-lactide, 0.08 mL of 1-BuOH (1.08 mmol), and 5 mL of toluene were charged into a 50 mL, three-necked, round-bottom flask connected to a dry N<sub>2</sub> purge. The flask was uniformly heated to 95°C with an oil bath and the reaction was magnetic stirred. After the dissolution of lactide in toluene solvent, 0.1 wt % of the Sn(Oct)<sub>2</sub> catalyst was transferred to the reaction kettle.

The same procedure was used for the synthesis of PLA initiated by choline and Ethoquad avoiding the use of 1-BuOH. The products were named PLA-Bu, PLA-CC, and PLA-Et, respectively, and were synthesized in order to evaluate the effect of the modifiers as ROP initiators.

PLA in the presence of clay was synthesized by 2.5 g of *rac*-lactide, 0.08 g of MMT-Na<sup>+</sup>, previously dried at 100°C in an oven for 12 h and 10 mL of toluene were charged into a 50-mL three-necked round-bottom flask connected to a dry N<sub>2</sub> purge.

After the reaction and re-precipitation, carried out as previously reported, the methanol-soluble polymer fraction was recovered by solvent removal.

The same procedure was used for the synthesis of PLA in the presence of MMT-Na<sup>+</sup> previously dried under reduced pressure (100°C, 0.01 bar) for 48 h, and pyrophyllite previously dried under reduced pressure (100°C, 0.01 bar) for 48 h. The latter was synthesized in order to investigate as neat charges of the clay can affect the ROP synthesis. The pyrophyllite structure is identical to the MMT one, but neat charges are absent. The products were named PLA-MMT-Na<sup>+</sup>, PLA-MMT-Na<sup>+</sup>-dry, and PLA-pyroph, respectively.

For the synthesis of the chitosan-based nanocomposite, the preparation of a masterbatch and the successive melt-blending with PLA was impossible because of the low thermal stability of chitosan. Therefore, a nanocomposite was prepared by using a lower amount of MMT-Ch (0.15 g) corresponding to 3 wt % directly by *in situ* polymerization. The sample was named as nanoChROP.

#### Preparation of nanocomposites by melt-blending of masterbatches and high molecular weight PLA

After drying at 60°C for 3 h under reduced pressure, PLA pellets were melt-blended with MasterC and MasterE in a counter-rotating internal mixer (Brabender type) at the constant rotation speed of 100 rpm for 20 min. Melt processing was carried out in a dry nitrogen atmosphere to prevent thermo-oxidative degradation of the PLA. The temperature was set at 180°C; however, it increased about 10°C during blending due to shearing processes. The two samples were named nanoCrop and nanoEtrop, respectively.

#### *In vitro* biodegradation

Each phosphate buffered saline (PBS) tablet was dissolved in 200 mL distilled water to obtain a solution consisting of 137 mM NaCl, 2.7 mM KCl, and 10 mM phosphate buffer (pH 7.4 at 25°C). Samples with weights ranging from 0.27 to 0.30 g were cut from about 2 mm thick film obtained by compression molding from the polymer materials obtained. The samples were separately immersed in 10 mL of PBS by using a plastic tube sealed with a cap and incubated in an oven at 60°C until removal after 2–10 weeks. The buffered solution was exchanged every 4 weeks.

At the end of each degradation time, the samples were removed from the solution, rinsed with distilled water, dried under reduced pressure (50°C, 0.01 bar) for 48 h, and weighed to determine the weight loss (each data point was the average of three samples).

At the end of 10 weeks, the samples were analyzed by size exclusion chromatography (SEC) to determine the final average molecular weight.

### Characterization techniques

$^1\text{H-NMR}$  spectra of polymers obtained from ROP carried out in the presence or not of clay were recorded on a Varian Unity VXR spectrometer at 300 MHz. Deuterated chloroform was used as the solvent (Euriso-top, 99.8%). DOSY maps were recorded on a 600 MHz spectrometer. Molecular weight of the samples obtained by ROP was calculated from the  $^1\text{H-NMR}$  spectra as the ratio between the integrals of the peaks at 1.55 ppm and 0.98 ppm, respectively.

FTIR spectra were recorded on a Perkin-Elmer 1760-X spectrometer. The polymeric material was analyzed by solution casting on KBr tablets, or by blending with KBr powder and successive compression to obtain tablets. The peaks were resolved with deconvolution operations using Lorentian equations to allow quantitative analysis.

UV-vis absorbance spectra were recorded at room temperature on a Perkin-Elmer Lambda 650 spectrophotometer using 1-cm path length quartz cells.

The average molecular weights ( $\overline{M}_n$ ,  $\overline{M}_w$ ) and polydispersity index ( $\overline{M}_w/\overline{M}_n$ ) of all PLA samples obtained were determined by SEC on a Jasco chromatograph equipped with PU-2089 Plus pump, two Mixed-D PLgel columns (7.5 mm  $\times$  300 mm), a PLgel precolumn (50 mm  $\times$  7.5 mm), a 2031 Plus RI detector, and a Jasco UV-2077 Plus detector. Chloroform elution rate was set at 1 mL/min. Each sample was filtered through a 0.2  $\mu\text{m}$  porosity filter.

The thermal stability of reagents, products, and composites was determined using a Mettler Toledo thermo-gravimetric analysis (TGA)/simultaneous differential *thermal analysis* (SDTA) 851<sup>e</sup> apparatus connected to a dry  $\text{N}_2$  purge onto samples of 7–15 mg. Each analysis was run from 25°C to 600°C with a scanning rate of 10 °C/min under nitrogen or oxidative atmosphere.

Differential scanning calorimeter (DSC) thermogram were recorded on a Mettler Toledo Star<sup>e</sup> System DSC 922<sup>e</sup> Module apparatus equipped with a CCA7 cooling system connected to the  $\text{N}_{2(0)}$  dewar. The samples (7–15 mg by weight) were heated to 220°C at a rate of 20 °C/min, cooled to 0°C and heated again. The second heating scans were run at 10 °C/min in order to determine crystallization, melting, and glass transition temperatures of the polymer. The under-cooling ( $\Delta T = T_m - T_c$ ) was calculated and used as a measure of the crystallization rate.

X-ray diffraction data of compression molded composites (2 mm thick) were collected with a D500/501 Siemens kristalloflex 810 diffractometer in Bragg-Brentano geometry. The data were collected in a range of  $2\theta = 2\text{--}30^\circ$  at steps of 5 s/scan.

Transmission electron microscopy (TEM), by means of a Zeiss EM900 microscope, was used to investigate nanostructure features of selected PLA-based composites. Ultra-thin sections (about 50 nm thick) were prepared at  $-80^\circ\text{C}$  by using a Leica EM FCS cryo-ultramicrotome equipped with a diamond knife. Samples directly obtained from melt blending or further compression molded were analyzed.

Melt flow rate (MFR) of all PLA samples obtained from ROP was determined with a CEAST PIN 7026 apparatus, at 190°C according to ISO1133A procedure. All samples were dried in vacuum at 60°C overnight before use.

Mechanical properties of PLA and PLA-based composites were studied with a Tinius Olsen H10KT dynamometer, equipped with a 500 N HTE charge cell. Samples were prepared according to ASTM D638 procedure using a dinking machine from the compression molded films and analyzed at room temperature with a stretch rate of 1 mm/min. Each data is the average of at least 10 specimens tested.

Test specimens, obtained from 0.2 to 0.5 mm thick films (for tensile tests) were prepared by processing the pellets on a Collin PM20/200 press, equipped with a water cooling system. Each sample was preheated to 200°C for 2 min under atmosphere pressure, compressed (5 MPa) for 1 min and finally quenched under pressure for 3 min.

## RESULTS AND DISCUSSION

### Preparation of organophilic layered silicates

The effect of solvent polarity was examined by intercalating 2-hydroxyethyl-trimethylammonium (choline), polyethyleneoxide(15)-(hydrogenated tallow)-ammonium or oligochitosan in between the layers of pristine MMT ( $\text{MMT-Na}^+$ ) both in aqueous and in water/propanol 50/50 v/v solution (Table II). The exchange degrees obtained are in all cases higher than 96% and no significant differences were observed as a function of solvent and cation polarity. The value of the basal spacing,  $d_{001}$ , obtained by X-ray analysis for all the OMMTs (Table II) indicates an expansion of the interlayer distance that depends both on exchange degree and steric hindrance of the intercalated organic cations. In particular, the intercalation of the more sterically hindered Ethoquad cation leads to an OMMT with the largest basal spacing. On the contrary, MMT modified with oligo(chitosan) cation showed the lowest increase in  $d_{001}$  because of its  $\beta$ -sheet structure, that is similar to that showed from chitin in acidic solutions. In fact the XRD pattern of a chitosan film shows a  $d_{001}$  spacing of 0.39 nm.<sup>29</sup> The calculated interlayer space in the MMT-Ch (0.36 nm), obtained by summing the  $d_{001}$  increase in montmorillonite interlayer distance

**TABLE II**  
Correlation Between Degree of Exchange and Basal Spacing of Montmorillonite

Sample	Medium	Organic cation	2θ (°) <sup>a</sup>	<i>d</i> <sub>001</sub> (nm) <sup>b</sup>	% NR <sub>4</sub> <sup>+</sup> <sup>c</sup>
MMT-Ch	H <sub>2</sub> O	oligochitosane	6.27	1.41	98
MMT-CC	H <sub>2</sub> O	choline chloride	6.19	1.43	97
MMT-CL	H <sub>2</sub> O	choline lactate	6.17	1.43	/
MMT-Et	H <sub>2</sub> O	Ethoquad	5.02	1.76	99
MMT-Na <sup>+</sup>	H <sub>2</sub> O	/	7.10	1.24	0
MMT-CC/PrOH	H <sub>2</sub> O/PrOH	choline chloride	6.30	1.40	96
MMT-Et/PrOH	H <sub>2</sub> O/PrOH	Ethoquad	5.02	1.76	99

<sup>a</sup> Diffraction angle.

<sup>b</sup> Basal spacing.

<sup>c</sup> Degree of exchange.

(1.41–1.24 = 0.17 nm) and the diameter reported for Na<sup>+</sup> cation (0.19 nm) is in good agreement with the intercalation of chitosan having a β-sheet structure.

### Nanocomposites by melt intercalation

The behaviors of torque and temperature profiles, obtained at 100 rpm for filled and unfilled PLA, as a function of blending time are compared in Figure 2. A gaseous nitrogen atmosphere was used to prevent thermo-oxidation of the PLA matrix. At the beginning of the blending process, all the samples show an increase in temperature, that is sharper (> 20°C) for neat PLA, nanoCh, and nanoEt and it is probably due to the friction exerted by blades during mixing. With the exception of nanoCL, the torque, that is related to the viscosity of the system, drops and after about 4 min of blending slightly decreases, showing the lowest final value. As a general rule, this behavior reflected the progress in homogenization of the system presumably combined with a partial decrease in molecular weight of the PLA.<sup>30</sup> In fact, the melt processing of PLA under nitrogen atmosphere affects molecular weight ( $\overline{M}_n$ ) and polydispersity index ( $\overline{M}_w/\overline{M}_n$ ) both of PLA melt processed and

extracted from the composites, as shown in Table III where molecular parameters ( $\overline{M}_n$ ,  $\overline{M}_w/\overline{M}_n$ ) and MFR are collected. In particular, for neat PLA, after melt processing, the  $\overline{M}_n$  decreased by 11%. This trend is observed also for PLA extracted from composites. The highest decrease in the molecular weight obtained for nanoCL suggests a possible degradation pathway due to the nucleophilic attack of lactate to the ester bonds of PLA. Moreover, from a preliminary visual examination, black macro-agglomerates are present only within the nanoCh composite. This is probably due to the fact that the thermal stability of oligo(chitosan lactate) present in between the clay layers is lower than the melting temperature of PLA matrix. As a consequence, the thermal degradation of chitosan during blending process gave the collapse of the lamellar structure of MMT.

XRD and TEM were used to provide essential information on the structure of the organoclay (OMMTs) dispersed within the PLA matrix. The position (2θ<sub>CuKα</sub>) and the Bragg distance (*d*) relative to the (001) peak, obtained from XRD diffractograms of the nanocomposites were collected in Table IV. By comparing *d*<sub>001</sub> values of the OMMTs before (Table II) and after (Table IV) the dispersion into the PLA matrix, it clearly appears that the inter-lamellar spacing do not significantly change. TEM images of nanoEt, nanoCC, and nanoCL composites taken on samples melt compressed are compared in Figure 3. A NanoCh representative picture is shown in Figure

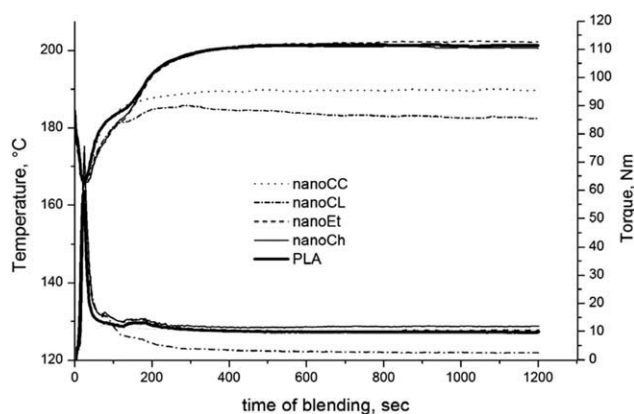


**Figure 2** Torque and temperature versus blending time recorded for nanocomposites nanoCL, nanoCC, nanoCh, nanoEt, and for neat PLA.

**TABLE III**  
Molecular Parameters for Processed PLA and Nanocomposites

Sample	Final torque	MFR	$\overline{M}_n$ (10 <sup>-3</sup> )	$\overline{M}_n$ decrease (%)	$\overline{M}_w/\overline{M}_n$
PLA	9.7	3.9 ± 0.2	120	11	1.7
NanoEt	10.4	6.7 ± 0.3	110	8	1.6
NanoCC	7.9	5.9 ± 0.3	103	14	1.7
NanoCL	2.5	33 ± 2	27	78	1.3
NanoCh	11.8	3.7 ± 0.3	140	-15	1.8

**TABLE IV**  
**Diffraction Maxima and Gallery Spacings for**  
**Compression Molded Samples nanoCC, nanoCL,**  
**nanoEt, and nanoCh**

Sample	$2\theta(^{\circ})$	$d_{001}(\text{nm})$
nanoMMTNa+	7.10	1.24
nanoCC	5.95	1.48
nanoCL	6.24	1.41
nanoEt	4.80	1.84
nanoCh	6.38	1.38

11(a). A high level of nanoclay delamination is observed for the nanoEt composite [Fig. 3(a,b)]: many multi-layered stacks and exfoliated layers, together with very few micro-aggregates are discernible within the PLA matrix. On the contrary, in the other two samples [Fig. 3(c,d)] the inorganic phase is arranged only in micro-agglomerates constituted by multi-layered stacks and in tactoids of sub-micrometric dimensions. The morphological findings obtained for the nanoEt sample are apparently in contrast with XRD results. However, it is important

to remind that XRD analysis provide information on ordered structures present into the bulk material, such as multi-layered stacks or aggregates, but it may not be able to pick up the presence of exfoliated layers or of tactoids constituted by few layers.

TGA (Table V) shows the starting degradation temperature ( $T_{\text{onset}}$ ) and the temperature of the maximum degradation rate ( $T_{\text{ip}}$ ) for neat PLA and the composites. The better dispersion of the silicate nanoplatelets observed in nanoEt does not affect the degradation process as  $T_{\text{onset}}$  and  $T_{\text{ip}}$  of this composite are not significantly different from those of neat PLA. Only nanoCh shows a  $T_{\text{ip}}$  higher than that of PLA, while nanoCL shows a very low  $T_{\text{onset}}$ . This can be ascribed to the low molecular weight of the polymer due to the high hydrolytic degradation that occurs during the blending process.

The effect of dispersion of clay particles on the crystallizability of PLA was investigated by DSC (Table V). For the composites, no significant changes in thermal properties are observed with respect to neat PLA. Thus, the expected plasticizing effect of poly(ethylene oxide) (PEO) chains, present in the

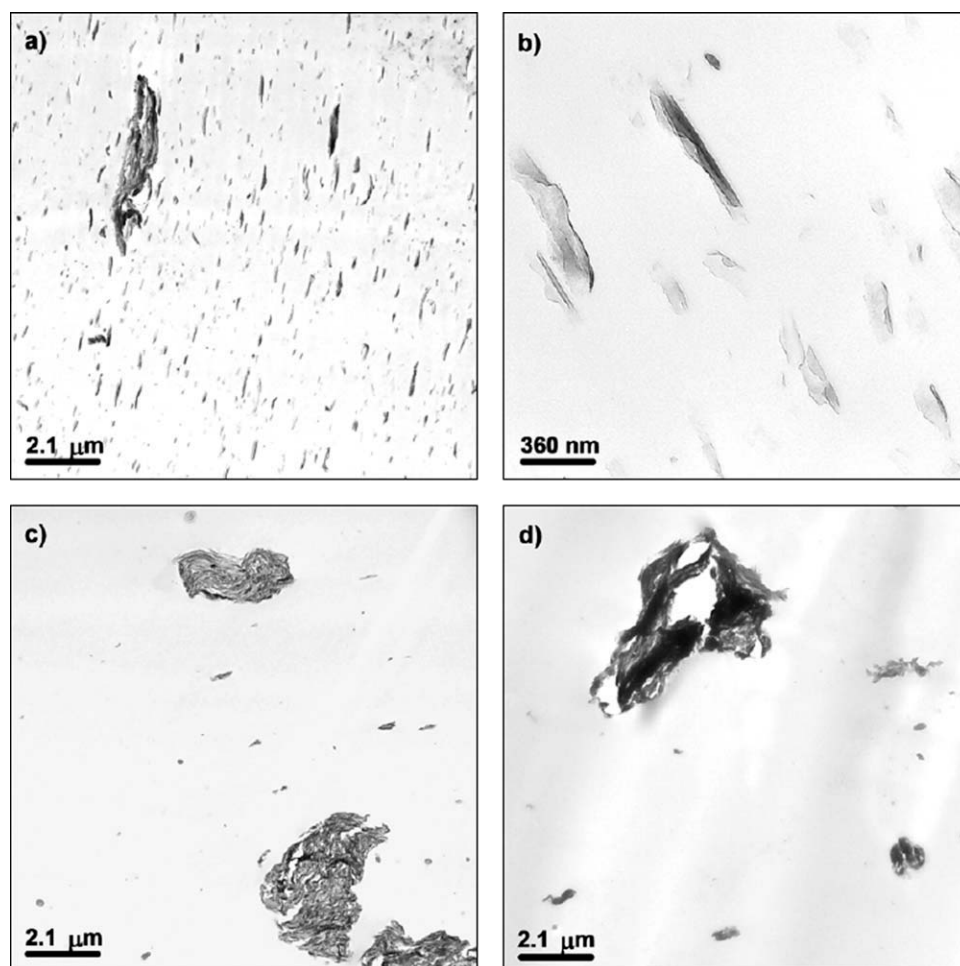


**Figure 3** TEM micrographs of samples: (a,b) nanoEt, (c) nanoCL, and (d) nanoCC.

**TABLE V**  
Thermal Properties of Neat and Filled PLA Tested in the Air

Sample	$T_{\text{onset}}^a$	$T_{\text{ip}}^b$	Weight loss (%)	$T_g^c$	$T_{\text{cc}}^d$	$T_m^e$	$\Delta H_{\text{cc}}^f$ (J/g)	$\Delta H_m^g$ (J/g)
PLA	344	361	99	63	126	153	-17	19
nanoCh	345	370	97	61	129	154	-12	12
nanoEt	345	365	97	60	130	154	-10	10
nanoCL	333	362	95	62	123	152	-22	22
nanoCC	345	363	98	60	118	148/155	-28	29

<sup>a</sup> Onset temperature obtained by TGA measurements.

<sup>b</sup> Inflection point temperature by TGA measurements.

<sup>c</sup> Glass transition temperature.

<sup>d</sup> Cold crystallization temperature.

<sup>e</sup> Melting temperature.

<sup>f</sup> Cold crystallization enthalpy.

<sup>g</sup> Melting enthalpy.

nanoEt sample, is not able to decrease the glass transition temperature of the polyester matrix. However, this occurs in a wider range of temperatures, as shown in Figure 4. Moreover, the very low crystallization temperature,  $T_{\text{cc}}$ , and the corresponding enthalpy,  $\Delta H_{\text{cc}}$ , obtained for nanoCL can be ascribed to the degradation of the PLA matrix. This behavior is common for short macromolecules which are able to organize themselves, assume ordered conformations and then crystallize.

The effect of the organoclays presence on the mechanical properties of PLA was investigated performing tensile tests (Table VI). The high value of the ratio between the elongation at break and at yield ( $\varepsilon_b/\varepsilon_y$ ) obtained for nanoEt is the most significant result and it can be ascribed to a slight plasticizer effect of the PEO chains of the surfactant<sup>31</sup> present in between OMMT layers. The dispersion of the clay in the polymer matrix does not affect the Young modulus, or at least no direct correspondence between these two parameters can be assessed. As expected, nanoCL shows the lowest elongation at break ( $\varepsilon_b$ ) because of the high brittleness of the degraded polymer. All these findings are in good agreements with the results obtained from the calorimetric analysis.

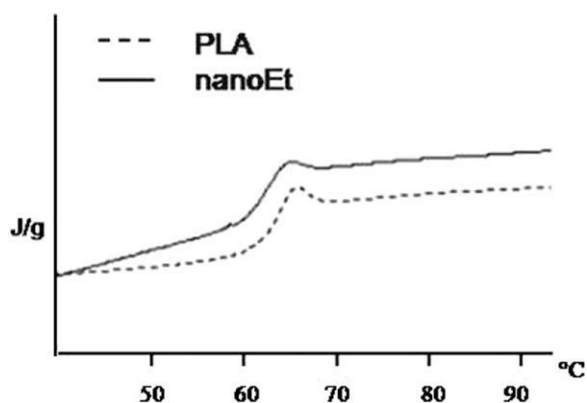


**Figure 4** Thermograms recorded for PLA and nanoEt.

To evaluate the effects of the different organoclays on the biodegradation rate of PLA, an *in vitro* hydrolytic degradation experiment was performed. Since the degradation rate of high molar mass PLA at 37°C is very low,<sup>32</sup> the experiment was performed at 60°C to accelerate the degradation process. Weight loss and final molecular weights after 10 weeks, as well as the kinetic constant and the enthalpy related to the biodegradation process, are collected in Table VII. For all the samples, there is a direct correspondence between the weight loss after 10 weeks in buffered solution and the final molecular weight of the residues. Moreover, the decrease in the molecular weight seems to be directly related to the weight loss. In fact, short polymer chains such as dimer, trimer, and lactic acid easily solubilize in phosphate buffered medium.<sup>33</sup>

As shown in Figure 5, where weight loss as a function of time is reported, the sample nanoCL showed the highest initial degradation rate because of the lowest polymer molecular weight. After that the degradation rate settled and became equal to that of the other samples.

The values of hydrolysis rate and final weight loss obtained for nanoCC and nanoEt samples (Table VII) are lower than of neat PLA with the same molecular weight in spite of the high hydrophilic

**TABLE VI**  
Mechanical Properties of Filled and Neat PLA

Sample	$E^a$ (MPa) $10^{-3}$	$\varepsilon_b^b$ (%)	$\sigma_y^c$ (MPa)	$\varepsilon_b/\varepsilon_y^d$
PLA	$3.0 \pm 0.2$	$27 \pm 5$	$62 \pm 4$	11
NanoCh	$3.1 \pm 0.1$	$3.4 \pm 0.9$	$53 \pm 3$	1.0
NanoEt	$2.7 \pm 0.2$	$4.3 \pm 1.1$	$51 \pm 5$	1.6
NanoCL	$3.3 \pm 0.4$	$1.1 \pm 0.1$	$20 \pm 3$	1.1
NanoCC	$2.5 \pm 0.1$	$4.2 \pm 0.7$	$55 \pm 2$	1.4

<sup>a</sup> Young modulus.

<sup>b</sup> Elongation at break.

<sup>c</sup> Strength at yield.

<sup>d</sup> Ratio between elongation at break and at yield.

**TABLE VII**  
**Weight Loss, Molecular Weight, and Kinetic Constant**  
**Resulting from Degradability Tests**

Sample	Weight loss (%)	Final $M_n(\times 10^{-3})$	$K$ (1/t)	$\Delta H_m$ (J/g)
PLA	52 ± 7	2.1	0.4	58
NanoCL	51 ± 7	2.3	0.3	56
NanoEt	49 ± 2	2.3	0.1	36
NanoCC	42 ± 4	2.6	0.1	45
NanoCh	41 ± 5	2.7	0.3	74

character of surfactants Ethoquad and choline. This is probably due to the low dispersion degree of the silicate sheets and consequently to the small interface area. DSC analysis showed high rate of cold crystallization during the first heating of both nanoCC and nanoEt. Since the hydrolytic degradation of polyester chains is known to take place in the amorphous phase of the matrix,<sup>34</sup> the higher is the crystallization rate of the composite, the lower is the hydrolysis extent. This phenomenon is expected to increase the PLA crystallinity. DSC analysis of the residues after 10 weeks of incubation confirmed the above theory. In fact, all the residues showed this theory total absence of cold crystallization peaks and a strong growth of melting enthalpy. Moreover, as shown in Figure 6, the overall opacity of the samples increases after 10 weeks of incubation in agreement with the evolution in crystallinity of the polymer matrix shown by DSC analysis.

#### Nanocomposites by *in situ* polymerization: Preliminary investigations

In the presence of Tin(II) octanoate, the polymerization of lactide to PLA takes place through the insertion of the monomer into the metal-oxygen bond of the initiator via selective cleavage of the acyl-oxygen bond of the lactide ring.<sup>11</sup> The presence of the clay seems to affect the final molecular weight of the polymer. Our preliminary studies of the polymerization reaction indicated that the presence of layered silicates gives lower molecular weight with respect to the pure polyester (Table VIII), as confirmed by the high solubility of the polymer matrix in methanol.

The values of molecular weight reported in Table VIII indicated that as the amount of coordination water in the inter-lamellar space increases, a higher number of shorter macromolecules are produced, leading to lower average molecular weight. This experimental finding is in agreement with previous works regarding the influence of organoclays having a controlled number of hydroxyl groups on the polymerization degree of poly( $\epsilon$ -caprolactone).<sup>19</sup> Indeed the ring opening initiation step can be started from various reactive groups on the surface of the clay, such as the silanol (Si—OH) groups. Moreover, the water molecules present in the

coordination spheres of sodium ions can act as co-initiator/chain transfer agents and also the inactivation of the initiator is possible.

In addition, the lamellar structure of the silicate itself could represent a physical obstacle to the propagation reactions. In fact, the synthesis of PLA on highly dried pyrophyllite, which is a neutral silicate with the same structure of MMT, gave a product with a molecular weight higher than that of PLA prepared in the presence of highly dried montmorillonite but still lower than that of pure PLA in spite of the absence of negative charges, enhancing nucleophilicity.

#### Nanocomposites by dilution of masterbatches prepared by *in situ* polymerization

By keeping into account the above described results, composites containing 30% by weight of organoclay (masterbatches) were prepared by *in situ* polymerization and then diluted in a high molecular weight PLA matrix by melt mixing. The two step-process is summarized in Figure 7.

In order to investigate the reaction mechanism, the activity of choline and Ethoquad as co-initiators for the ring opening of lactide was tested by carrying out these reactions with the two ammonium salts instead of the usually used co-initiator 1-BuOH. The presence of both reagent and product (polylactide) was evidenced by infrared analysis in the product recovered from the reaction initiated by choline,

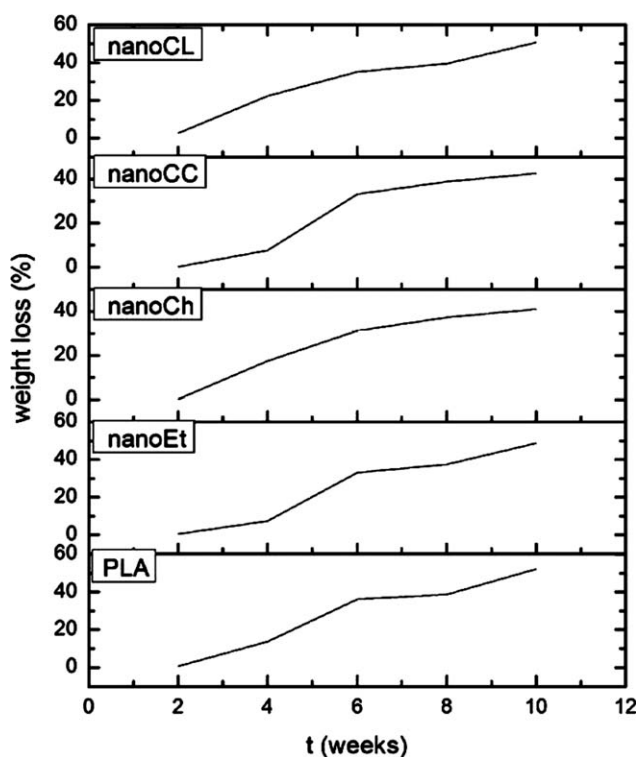


**Figure 5** Weight loss as a function of time for compression molded samples.

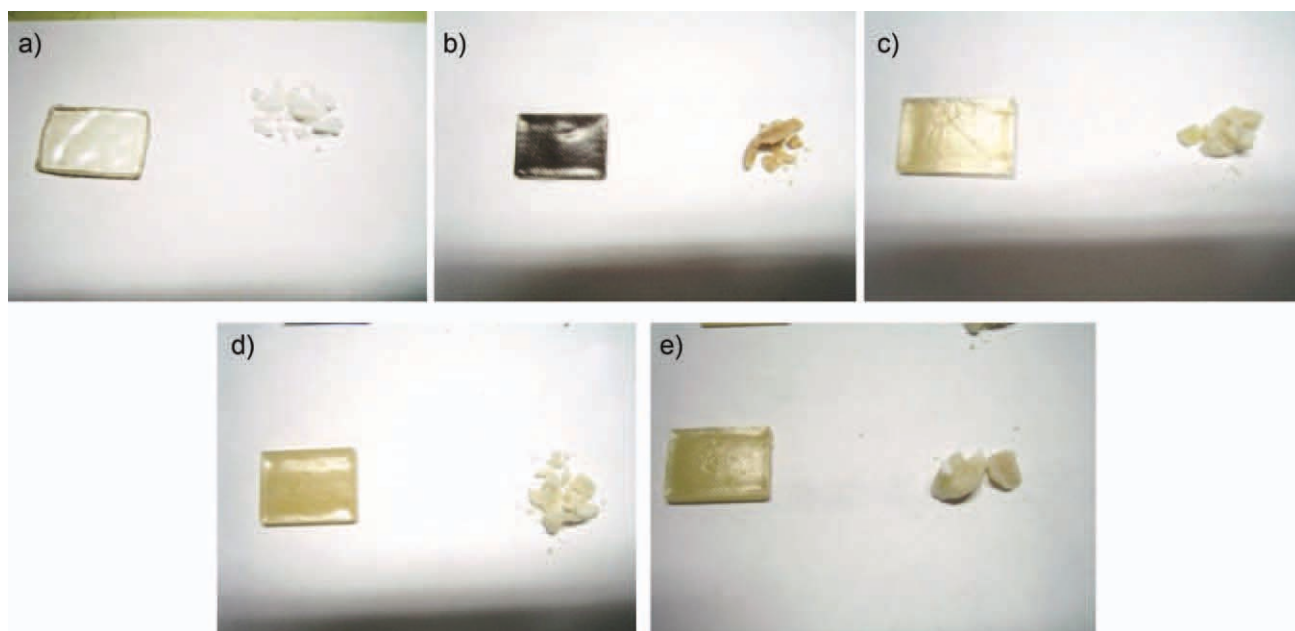


**Figure 6** Changes in sample visual aspect upon 10 weeks of hydrolysis for: (a) the PLA matrix; (b) nanoCL; (c) nanoEt; (d) nanoCC; (e) nanoCh. [Color figure can be viewed in the online issue, which is available at [wileyonlinelibrary.com](http://wileyonlinelibrary.com).]

and 600 MHz  $^1\text{H-NMR}$  spectroscopy coupled with the DOSY technique confirmed the occurrence of the polymerization. A molecular weight of 2,900 (corresponding to an average polymerization degree of 40) was determined from the integral value of the corresponding “d” and “a” protons (Fig. 8). A similar analysis carried out onto the product of the polymerization initiated by Ethoquad showed various molecular species (Fig. 9), whose diffusion coefficient was lower than the one recorded for neat Ethoquad ( $0.99 \times 10^{-10} \text{ m}^2/\text{s}$  in water). As a consequence, this product should contain a fragment coming from the ammonium salt. By analyzing the signals of the  $^1\text{H-NMR}$  and IR spectra, the most reasonable hypothesis for the structure of the main product is reported in Figure 9. Anyway, both the ammonium salts resulted to be active as initiator of the lactide ROP.

Hence, once the reactivity of choline and Ethoquad was confirmed, the two corresponding composites at high OMMT content were prepared and named MasterE and MasterC, respectively. A masterbatch containing unmodified nanoclay (PLA-MMT- $\text{Na}^+$ ) was also prepared as a reference. As well as the results

obtained for PLA-MMT- $\text{Na}^+$ , the polymer matrix present in the sample PLA-MMT-CC resulted partially soluble in methanol. FTIR analysis revealed that the amount of PLA in the insoluble fraction was 10% by weight. This value was evaluated by using a proper calibration curve obtained by analyzing the spectra of PLA/MMT- $\text{Na}^+$  composites containing various amounts of clay: the ratio between the areas of the bands at  $1752$  and  $1050 \text{ cm}^{-1}$ , corresponding to PLA matrix and silicate respectively, was plotted as a function of PLA content. Moreover, the composite was subjected also to extraction by chloroform. The analysis of both soluble and insoluble fractions through SEC showed quite similar molecular weights (1818 Da). As a consequence, the insolubility can be ascribed to interactions between the polyester and the organic surfactant of MMT not involving all the PLA polymeric chains as it was possible to extract a consistent amount of polymers, thanks to its solubility in chloroform.

PLA-MMT-Et showed a quite similar behavior, even if the amount of PLA in the insoluble fraction was higher (20 wt %) than that obtained for PLA-MMT-CC. As mentioned above, the real structure of the product is not yet known, so it was not possible to determine the molecular weight of the two polymer fractions by  $^1\text{H-NMR}$  analysis. To verify the presence of interactions between the polymer and the organic surfactant of montmorillonite, the composite was extracted with hot methanol and the resulting insoluble fraction was tentatively further extracted with chloroform. FTIR analysis of the extract revealed the absence of polymer, then it was possible to assert that PLA and Ethoquad strongly interact with the MMT.

**TABLE VIII**  
Molecular Weight and Polymerization Degree of Pure PLA Prepared by ROP and of PLA Prepared in the Presence of Montmorillonite and Pyrophillite

Sample	$M_n (\times 10^{-2})$	$DP_n$
PLA-Bu	52	72
PLA-MMT- $\text{Na}^+$	7	10
PLA-MMT- $\text{Na}^+$ -dry	13	17
PLA-pyroph	19	26

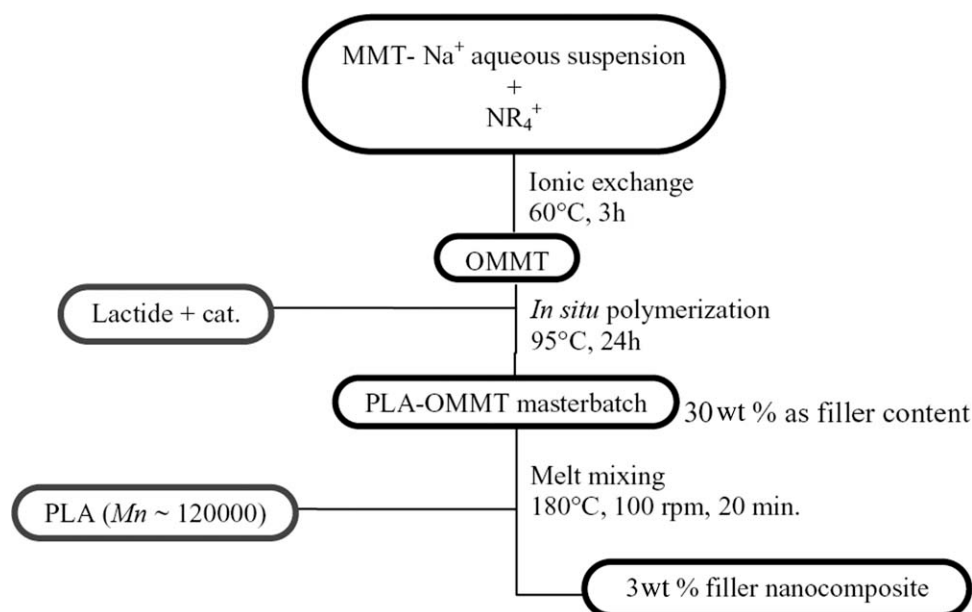
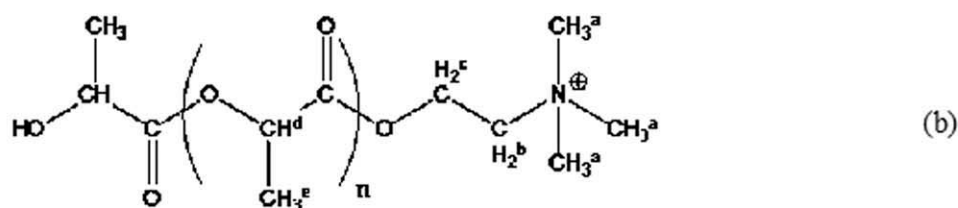
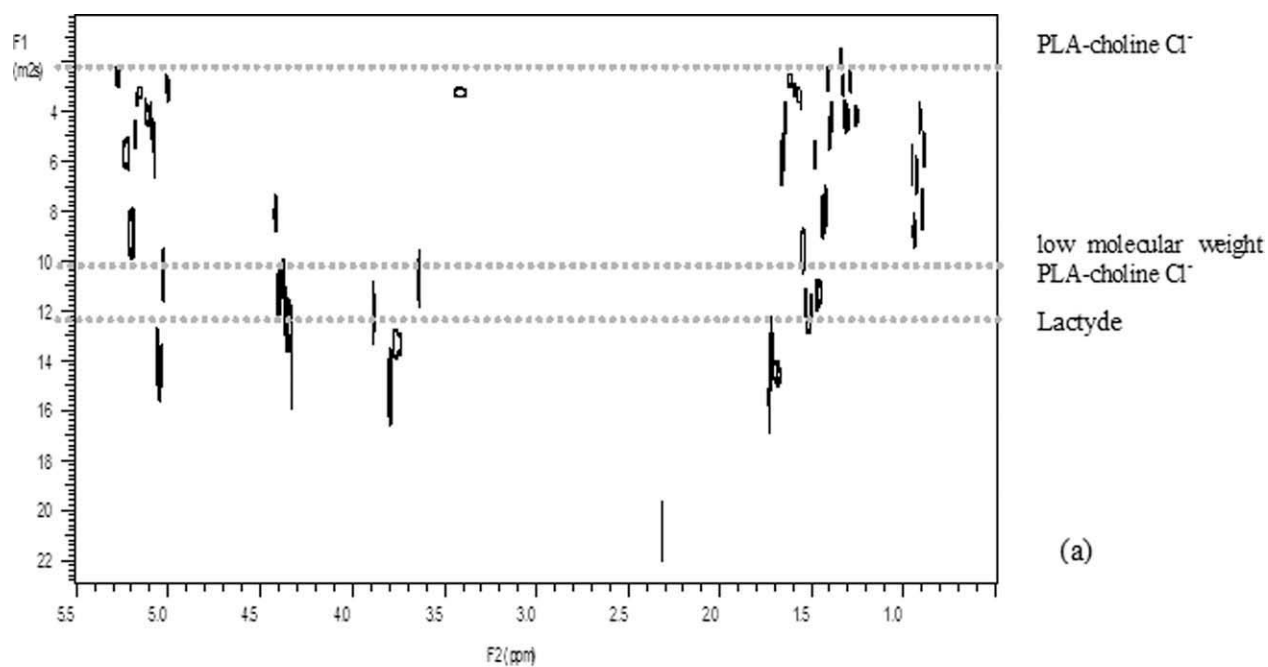


**Figure 7** Scheme of the preparation of PLA/OMMT nanocomposites through the use of a masterbatch prepared by ROP polymerization onto OMMT.



<sup>1</sup>H NMR (600 MHz, CDCl<sub>3</sub>) δ 5.20 (q, 25H, H<sub>d</sub>), 4.8 (s, 1H, H<sub>c</sub>), 4.5 (s, 1H, H<sub>c</sub>), 4.25 (s, 1H, H<sub>b</sub>), 4.09 (s, 1H, H<sub>b</sub>), 3.4 (s, 6H, H<sub>e</sub>), 1.5 (d, 75H, H<sub>a</sub>). *M<sub>n</sub>* = 2900, *D* = 3.5 · 10<sup>-10</sup> m<sup>2</sup>/s

**Figure 8** (a) DOSY map and (b) choline-initiated PLA structure, <sup>1</sup>H-NMR signals, molecular weight, and diffusion coefficient.

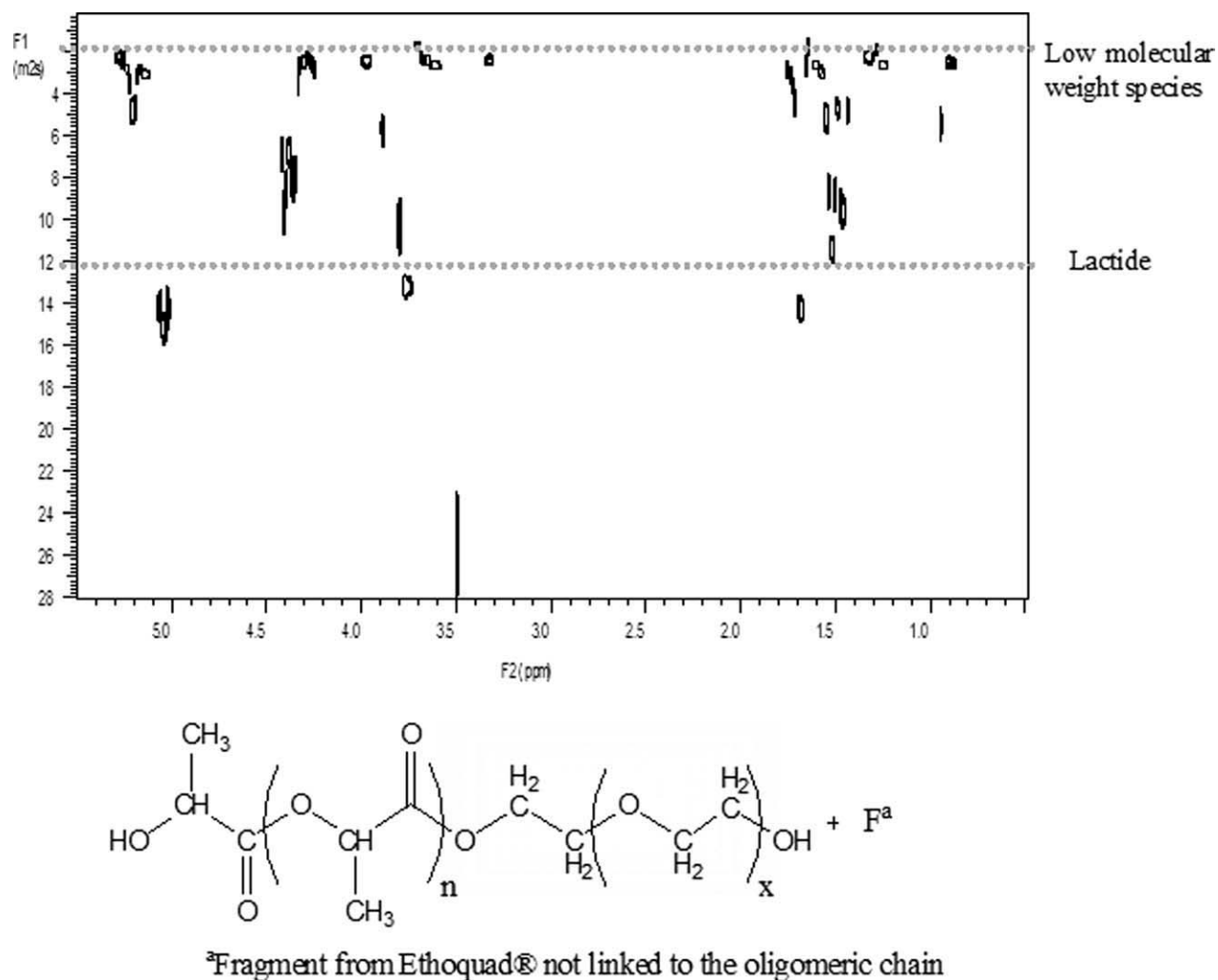


Figure 9 (a) DOSY map and (b) hypothesis of Ethoquad-initiated PLA structure.

After characterization, PLA-MMT-Et and PLA-MMT-CC were further melt blended with high molecular weight PLA by using an internal mixer. Two different 3 wt % PLA/OMMT composites were obtained and named nanoEtMaster and nanoCCMaster, respectively. PLA processed in the same experimental conditions was taken as a reference.

In Table IX the molecular parameters obtained by SEC and the MFR for these samples are collected. By melt processing PLA with the masterbatches that contain oligomeric species, the molecular weight of the polymer matrix extracted from the sample nanoCCmaster strongly decreased with respect to that of neat PLA, while that from nanoEtmaster remains practically the same. Moreover, the values of MFR and final torque are in good agreement with these findings.

As already observed for nanoEt and nanoCC samples, the XRD analysis of these nanocomposites indicated that the basal spacing remained practically the same of those measured for the organoclays before the dispersion into the PLA matrix (Table II vs.

Table X). No evidences of intercalation of polymer chains in between clay layers were obtained.

Figure 10 shows examples of TEM images taken on nanoEtMaster and nanoCCMaster. In the first sample, a small fraction of submicrometric agglomerates and a large number of stacks containing few sheets and of isolated layers are discernible [Fig. 10(a,b)]. On the other hand, TEM images of nanoCCMaster reported in Figure 10(c,d) show stacks having a smaller average size than that of the inorganic particles in nanoCC.

TABLE IX  
Molecular Parameters for Processed  
PLA and Nanocomposites

Sample	Final Torque (N m)	MFR	$M_n$	$M_n$ decrease (%)	$M_w/M_n$
PLA	9.7	$3.9 \pm 0.2$	$107 \times 10^3$	11	1.7
nanoEtMaster	7.9	$13.4 \pm$	$102 \times 10^3$	15	1.7
nanoCCMaster	4.4	$42.1 \pm 0.3$	$75 \times 10^3$	38	1.8

**TABLE X**  
**Diffraction Peaks and Gallery Spacings for**  
**Compression Molded Samples nanoCCMaster**  
**and nanoEtMaster**

Sample	2 $\theta$ (°)	$d_{001}$ (nm)
nanoCCMaster	6.06	1.46
nanoEtMaster	4.80	1.84

**PLA/chitosan-modified montmorillonite nanocomposite by *in situ* polymerization**

Because of the low thermal stability of chitosan, it was not possible to use the two step-process applied for the preparation of nanocomposites containing MMT modified with choline chloride and Ethoquad. Therefore, the nanocomposite nanoChROP was directly prepared by ROP of lactide inside the interlamellar spacing of MMT modified with chitosan (MMT-Ch) with a MMT content of 3% by weight.

The determination by  $^1\text{H-NMR}$  of the molecular weight was made difficult because of the complex structure of the obtained polymer. However, its total insolubility in methanol means that the molecular weight is probably similar or higher than that of PLA prepared by ROP. Moreover, also the possibility of obtaining brush-like structures characterized by short PLA chains grafted onto chitosan, as evidenced in papers dealing with the ROP of lactide onto chitosan,<sup>35,36</sup> can be invoked.

From XRD analysis, the  $d_{001}$  of the organoclay increased from 1.3 nm of MMT-Ch to 1.6 nm of nanoChROP and the peak broadened, indicating the possible presence of polymer chains in the galleries of the clay. Anyway the TEM analysis, made difficult by the high brittleness of the sample, showed the presence of agglomerates with a micrometric size, usually bigger than the ones observed in the NanoCh sample (Fig. 11).

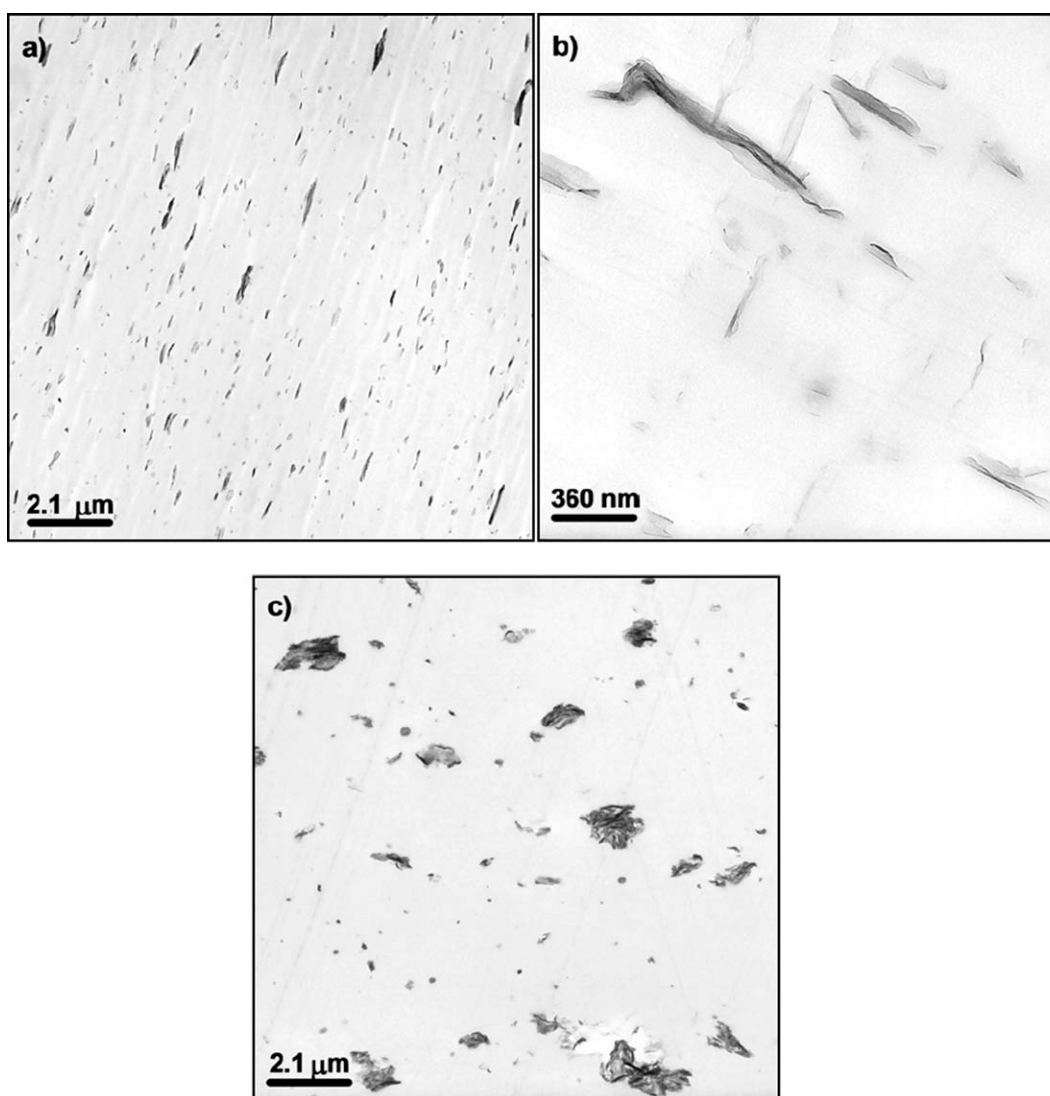


**Figure 10** TEM micrographs of samples: (a,b) nanoEtMaster; (c) nanoCCMaster.

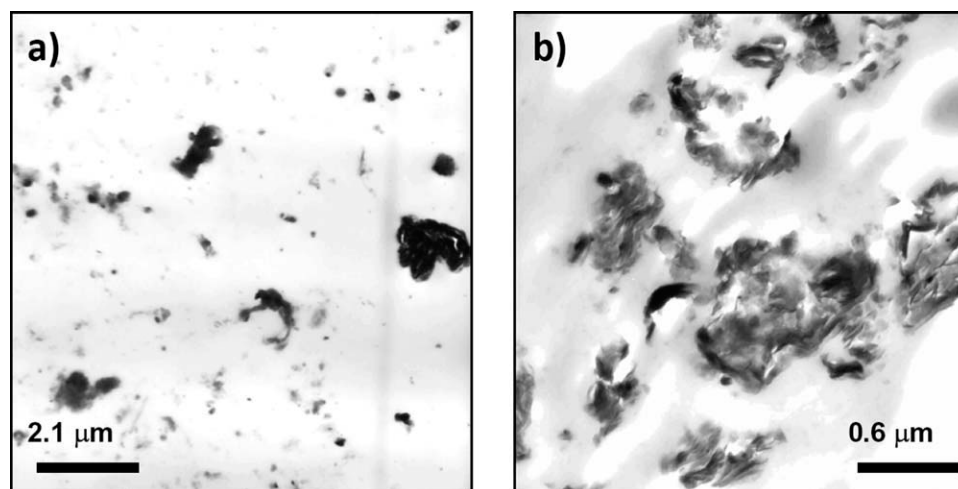


**Figure 11** TEM micrographs obtained by analyzing NanoCh (a) e NanoChMaster (b).

Thermal analysis of nanoChROP and pure PLA prepared by ROP revealed a sharp increase in the thermal stability due to the MMT-Ch dispersion as  $T_{i,p}$  increased from 281 for pure PLA-Bu, synthesized by ROP, to 295°C for nanoChROP.

### CONCLUSIONS

In the present study, different aspects of the preparation of PLA/OMMT nanocomposites were kept into account.

- The ion exchange experiments allowed to easily replace  $\text{Na}^+$  with potentially biocompatible cations, not yet employed for such application. The ion exchange study showed a relationship between the degree of exchange and the basal spacing  $d_{001}$  of montmorillonite. The latter increased when an increased degree of exchange was achieved, steric hindrance of intercalated ions being equal.
- The melt blending of PLA with Ethoquad or choline chloride modified montmorillonite (MMT-Et and MMT-CC, respectively) allowed the preparation of two composites with a partially intercalated nanostructure and a microstructured morphology, respectively.
- From the preliminary investigations of ROP of lactide it was demonstrated that the synthesized PLA had a lower molecular weight with respect to the commercial one. Moreover the presence of layered silicates in the bulk affected the final molecular weight of the polymer producing a lower molecular weight material with respect to the synthesis of pure polyester. The presence of

neat charges onto the layers gave a further contribution in decreasing the molecular weight.

- As the molecular weight of PLA prepared by ROP was too much low to grant appreciable mechanical properties, a two step method was adopted by previously preparing by ROP a composite with a 30 wt % OMMT content and then diluting it in the mixer by adding commercial PLA up to 3 wt % of OMMT content. The morphology of the nanocomposites prepared by the two-step route resulted improved with respect to the melt-blended samples, but on the other hand, the tensile modulus and thermal stability seemed to be worse. They were probably affected by the presence of the low molecular weight PLA fraction coming from the *in situ* polymerization.
- Anyway although the improvement of mechanical and thermal properties was negligible, our investigation evidenced that preliminary preparation of an inorganic-rich masterbatch through *in situ* polymerization of lactide gave rise to a good dispersion of the inorganic phase, thanks to the strong interactions between the OMMT and the polymer matrix. Hence this method should be further investigated in order to reach a better control of the PLA structural features depending on the polymerization routes and conditions.
- The preparation of nanocomposites by using chitosan lactate as possible modifier for  $\text{MMT-Na}^+$  resulted difficult as the melt blending of chitosan modified montmorillonite (Ch-MMT) in PLA resulted in degradation of chitosan, whereas the preparation by ROP of a 3% by weight Ch-MMT

composite resulted in appreciable thermal stabilization with respect to PLA prepared by ROP but in a coarse and irregular morphology, probably responsible, together with the low molecular weight of PLA, of the brittleness of the sample.

Prof. Gloria Uccello Barretta is thanked for scientific support about NMR techniques.

## References

- Lunt, J. *Polym Degrad Stab* 1998, 59, 145.
- Yu, L.; Dean, K.; Li, L. *Prog Polym Sci* 2006, 31, 576.
- Auras, R.; Harte, B.; Selke, S. *Macromol Biosci* 2004, 4, 835.
- Sorrentino, A.; Gorrasi, G.; Vittoria, V. *Trends Food Sci Technol* 2007, 18, 84.
- Coltelli, M.-B.; Della Maggiore, I.; Bertoldo, M.; Signori, F.; Bronco, S.; Ciardelli, F. *J Appl Polym Sci* 2008, 110, 1250.
- Masirek, R.; Kulinski, Z.; Chionna, D.; Piorowska, E.; Pracella, M. *J Appl Polym Sci* 2007, 105, 255.
- Serizawa, S.; Inoue, K.; Iji, M. *J Appl Polym Sci* 2006, 100, 618.
- Ray, S. S.; Bousmina, M. *Prog Mater Sci* 2005, 50, 962.
- Lecomte, P.; Riva, R.; Jerome, C.; Jerome, R. *Macromol Rapid Commun* 2008, 29, 982.
- Kamber, N. E.; Jeong, W.; Waymouth, R. M.; Pratt, R. C.; Lohmeijer, B. G. G.; Hedrick, J. L. *Chem Rev* 2007, 107, 5813.
- Albertsson, A. C.; Varma, I. K. *Biomacromolecules* 2003, 4, 1466.
- Finne, A.; Albertsson, A.-C. *J Polym Sci Part A: Polym Chem* 2003, 41, 1296.
- Coudane, J.; Ustariz-Peyret, C.; Schwach, G.; Vert, M. *J Polym Sci Part A: Polym Chem* 1997, 35, 1651.
- Frediani, M.; Sémeril, D.; Mariotti, A.; Rosi, L.; Frediani, P.; Rosi, L.; Matt, D.; Toupet, L. *Macromol Rapid Commun* 2008, 29, 1554.
- Dechy-Cabaret, O.; Martin-Vaca, B.; Bourissou, D. *Chem Rev* 2004, 104, 6147.
- Kubies, D.; Pantoustier, N.; Dubois, P.; Rulmont, A.; Jerome, R. *Macromolecules* 2002, 35, 3318.
- Lepoittevin, B.; Pantoustier, N.; Devalckenaere, M.; Alexandre, M.; Kubies, D.; Calberg, C.; Jerome, R.; Dubois, P. *Macromolecules* 2002, 35, 8385.
- Lepoittevin, B.; Pantoustier, N.; Alexandre, M.; Calberg, C.; Jerome, R.; Dubois, P. *J Mater Chem* 2002, 12, 3528.
- Chrissafis, K.; Antoniadis, G.; Paraskevopoulos, K. M.; Vassiliou, A.; Bikiaris, D. N. *Compos Sci Technol* 2007, 67, 2165.
- Paul, M.-A.; Alexandre, M.; Degee, P.; Calberg, C.; Jerome, R.; Dubois, P. *Macromol Rapid Commun* 2003, 24, 561.
- Lee, S.; Kim, C. H.; Park, J.-K. *J Appl Polym Sci* 2006, 101, 1664.
- Di, Y.; Iannace, S.; Di Maio, E.; Nicolais, L. *J Polym Sci Part B: Polym Phys* 2005, 43, 689.
- Feijoo, J. L.; Cabedo, L.; Gimenez, E.; Lagaron, J. M.; Saura, J. *J Mater Sci* 2005, 40, 1785.
- Pluta, M. *J Polym Sci Part B: Polym Phys* 2006, 44, 3392.
- Pluta, M.; Jeszka, J. K.; Boiteux, G. *Eur Polym J* 2007, 43, 2819.
- Pluta, M.; Galeski, A.; Alexandre, M.; Paul, M. A.; Dubois, P. *J Appl Polym Sci* 2002, 86, 1497.
- Gu, S.-Y.; Ren, J.; Dong, B. *J Polym Sci Part B: Polym Phys* 2007, 45, 3189.
- Lewitus, D.; McCarthy, S.; Ophir, A.; Kenig, S. *J Polym Environ* 2006, 14, 171.
- Blackwell, J.; Minke, R.; Gardner, K. H. Department of Macromolecular Science. Case Western Reserve University: Cleveland, OH, USA, 1978; pp 108–123.
- Signori, F.; Coltelli, M.-B.; Bronco, S. *Polym Degrad Stab* 2009, 94, 74.
- Sheth, M.; Kumar, R. A.; Dave, V.; Gross, R. A.; McCarthy, S. P. *J Appl Polym Sci* 1997, 66, 1495.
- Funabashi, M.; Ninomiya, F.; Kunioka, M. *J Polym Environ* 2007, 15, 245.
- Paul, M. A.; Delcourt, C.; Alexandre, M.; Degee, P.; Monteverde, F.; Dubois, P. *Polym Degrad Stab* 2005, 87, 535.
- Thellen, C.; Orrotha, C.; Froio, D.; Ziegler, D.; Lucciarini, J.; Farrell, R.; D'souza, N. A.; Ratto, J. A. *Polymer* 2005, 46, 11716.
- Liu, Y.; Tian, F.; Hu, K. A. *Carbohydr Res* 2004, 339, 845.
- Luckachan, G. E.; Pillai, C. K. S. *Carbohydr Polym* 2006, 64, 254.